Radicals

Deutsche Ausgabe: DOI: 10.1002/ange.201605612
Internationale Ausgabe: DOI: 10.1002/anie.201605612

The Planar Blatter Radical: Structural Chemistry of 1,4-Dihydrobenzo[*e*][1,2,4]triazin-4-yls

Piotr Kaszyński, Christos P. Constantinides, and Victor G. Young, Jr.*

Abstract: *Two planarized analogues of the prototypical Blatter radical (**1**), peri-annulated **1$_S$** and **1$_O$**, are demonstrated and provide a new platform for molecular and supramolecular engineering, and for tuning electronic and magnetic properties of the radical. Planarization of **1** results in bathochromic shift to the near-IR region, greater spin delocalization, and anodic shift of the reduction potential only for **1$_S$**. Magnetization studies revealed nearly ideal paramagnetic behavior at high temperatures for both radicals **1$_S$** and **1$_O$** with one-dimensional ferromagnetic interaction in the former ($2J = 14.4\ cm^{-1}$) and antiferromagnetic interactions in **1$_O$** at low temperatures.*

Recent years have witnessed rapid progress in the chemistry of the benzo[*e*][1,2,4]triazin-4-yl radical[1] driven by the prospect of its applications in contemporary technologies. Thus, the exceptional stability,[2] spin π-delocalization,[3] narrow electrochemical window,[4] and low excitation energies[5] made benzo[*e*][1,2,4]triazin-4-yl derivatives, such as **1** (Figure 1),[6] attractive for application in controlled polymerization,[7] molecular electronics,[8] photodetectors,[9] and liquid crystalline photoconductors.[10] In this context several synthetic methods for accessing this radical system have been recently improved[11] and developed,[4a,12] and transformations of functional groups in the presence of the unpaired electron demonstrated.[5b] In addition, the planar π system has been extended by annulation at positions 6–7[4b,9,13] and 7–8[14] of the prototypical Blatter radical **1**, thus providing access to new materials with tunable properties. Many of these derivatives have also been investigated for solid-state magnetic behavior showing relatively strong antiferromagnetic[13a,c,14,15] and ferromagnetic[13a,15c,16] interactions.

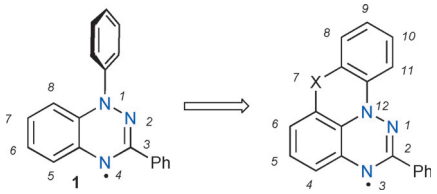

Figure 1. Conceptual transformation of the Blatter radical **1** into its planar analogues **1$_S$** (X = S) and **1$_O$** (X = O). The numbering system for each heterocycle is shown.

The general feature of all benzo[*e*][1,2,4]triazin-4-yl derivatives known to date is the presence of an aryl substituent at the N1 position, such as Ph in **1**, which due to steric interactions between the C8–H and C(*ortho*)–H forms a large dihedral angle θ with the heterocycle, for example, for 1-Ph θ is in a range of 38[13a]–82°[16c] (avg. 59° ± 13°).[4b,13a,b,15c,16c,17] This high torsional angle between the π planes limits spin delocalization from N1, with the highest spin density,[3] and affects molecular packing in the solid state, which in turn impacts magnetic properties of the solids. A coplanar π substituent at N1 would provide maximum spin delocalization, change in packing of the solid state, and offer a new platform for the design of functional materials.

The most effective way to planarize **1** appears to be the connection of the C8 and C(*ortho*) positions with a chalcogen, such as sulfur or oxygen in structures **1$_S$** and **1$_O$** (Figure 1). Now we describe a simple and potentially wide-scope method for the preparation of planarized Blatter radical. We report the synthesis, complete characterization by XRD, spectroscopic, electrochemical, magnetic and computational methods, and compare these results with those for **1**.

Radicals **1$_S$** and **1$_O$** were obtained in a typical yield of 20–30% using our recently developed method[12] by reacting the benzo[*e*][1,2,4]triazine **2$_S$** and **2$_O$**, respectively, with *t*BuLi, followed by aerial oxidation of the intermediate anion and chromatographic purification of the final product (Scheme 1). The triazines **2** were conveniently prepared by nucleophilic aromatic substitution of fluorine in 8-fluorobenzo[*e*]-[1,2,4]triazine (**3**) with either 2-bromothiophenoxide or 2-bromophenoxide under phase-transfer catalysis conditions. The triazine **3** was prepared in three steps and 76% overall yield from benzhydrazide, which was N-arylated with 2,3-difluoronitrobenzene to form the hydrazide **4** with subsequent cyclization to **3** under reductive conditions. Details are provided in the Supporting Information.

Single-crystal XRD analysis revealed that annulation of **1** with a sulfur atom reduced the Ph-N1 torsional angle $\theta_{C\text{-}C\text{-}N\text{-}N}$ from 50.6° in **1**[17c] to 7.5° in **1$_S$**, while the central phenothiazine ring is puckered along the S···N line by 16.0°, presumably

[*] Prof. Dr. P. Kaszyński
Center for Molecular and Macromolecular Studies
Polish Academy of Sciences, Sienkiewicza 112, 90-363 Łódź (Poland)
and
Department of Chemistry, Middle Tennessee University
Murfreesboro, TN 37123 (USA)
and
Faculty of Chemistry, University of Łódź
Tamka 12, 91-403 Łódź (Poland)
E-mail: piotrk@cbmm.lodz.pl
Dr. C. P. Constantinides
Department of Chemistry, North Carolina State University
Raleigh, NC 27695 (USA)
Dr. V. G. Young, Jr.
X-ray Crystallographic Laboratory, Department of Chemistry
University of Minnesota, Twin Cities, MN 55455 (USA)
Supporting information and the ORCID identification number(s) for the author(s) of this article can be found under:
http://dx.doi.org/10.1002/anie.201605612.

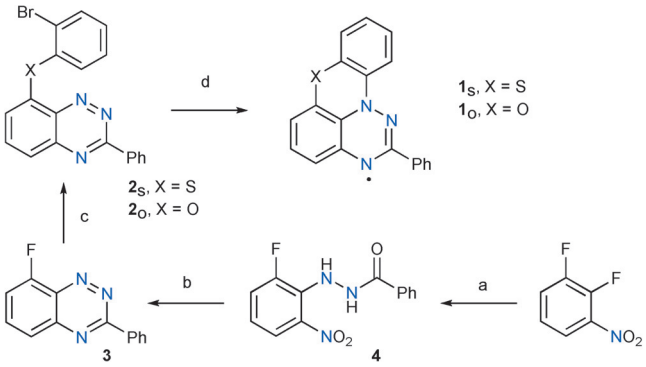

Scheme 1. Synthesis of benzo[*e*][1,2,4]triazin-4-yl derivatives $\mathbf{1_S}$ and $\mathbf{1_O}$. Reagents and conditions: a) $PhCONHNH_2$, DMSO, 100 °C, 14 h; b) 1. Sn, AcOH, RT 1.5 h, then 20 min at 120 °C; 2. $NaIO_4$, CH_2Cl_2/MeOH (1:1); c) 2-BrC_6H_4SH (for $\mathbf{2_S}$) or 2-BrC_6H_4OH (for $\mathbf{2_O}$), K_2CO_3, $[NBu_4]^+Br^-$, MeCN, reflux 3–5 h; d) 1. *t*BuLi, THF, −78 °C; 2. air. DMSO = dimethylsulfoxide, THF = tetrahydrofuran.

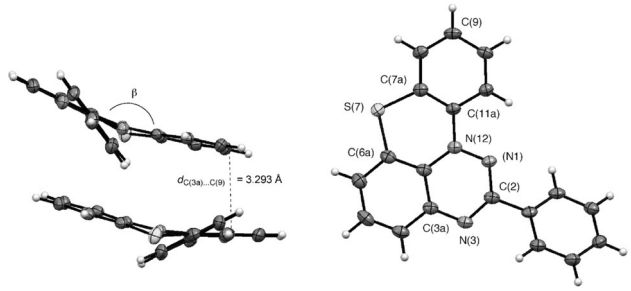

Figure 2. Thermal ellipsoid diagram for $\mathbf{1_S}$ (ellipsoids shown at 50% probability). Labels according to the chemical structure. Left: short intermolecular contact C3a···C9. Right: selected intramolecular dimensions: N(1)-N(12) = 1.368(3) Å, N(12)-C(11a) = 1.420(3) Å, N(1)-C(2) = 1.331(3) Å, S(7)-C(6A) = 1.757(3) Å, C(6a)-S(7)-C(7A) = 101.53(13)°, ring interplanar β = 164.0°. For other molecular dimensions and details see the Supporting Information.

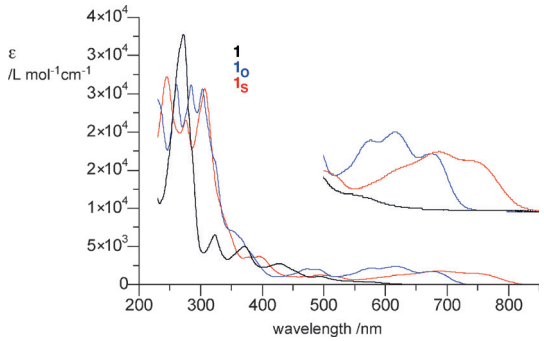

Figure 3. UV/Vis spectra for the Blatter radical **1** (dotted line), $\mathbf{1_O}$ (dashed line) and $\mathbf{1_S}$ (solid line) in CH_2Cl_2. The inset shows enlarged region 500–850 nm.

because of the long C–S bonds (Figure 2). DFT calculations reproduced well the experimental structure of $\mathbf{1_S}$ and showed that the planar C_s-symmetric structure represents a first-order transition state for ring inversion and is higher by $\Delta H =$ 0.46 kcal mol^{-1} than the puckered ground-state.

The structure of fine hairlike crystals of the oxygen analogue $\mathbf{1_O}$ was obtained with a synchrotron light source. It shows essentially planar molecules (mean deviation from the plane 0.0256 Å) arranged equidistantly (3.390 Å) into π-slipped stacks and forming a 56.7° angle with molecules in the neighboring stacks. The experimental molecular geometry is consistent with the DFT-calculated planar, C_s-symmetric ground-state structure for $\mathbf{1_O}$.

Peri-annulation of **1** resulted in significant bathochromic and hyperchromic shifts, particularly of the low-energy electronic absorption bands: the lowest energy band in the spectrum of $\mathbf{1_O}$ is shifted by 134 nm (−0.46 eV) to 675 nm and by 200 nm (−0.62 eV) to 740 nm in the spectrum of $\mathbf{1_S}$, relative to that in the spectrum of **1** (Figure 3). Interestingly, TD-DFT calculations in the CH_2Cl_2 dielectric medium revealed that the SOMO→α-LUMO transition in **1** is little affected by peri-annulation with a sulfur atom ($\Delta E = +11$ meV for $\mathbf{1_S}$) and modestly shifted to lower energies in $\mathbf{1_O}$ ($\Delta E = -93$ meV). In contrast, the β-HOMO→β-LUMO transition is significantly affected by peri-annulation ($\Delta E = -631$ meV for $\mathbf{1_S}$ and $\Delta E = -447$ meV for $\mathbf{1_O}$) and apparently responsible for the near-IR absorption observed in $\mathbf{1_S}$ (Figure 4).

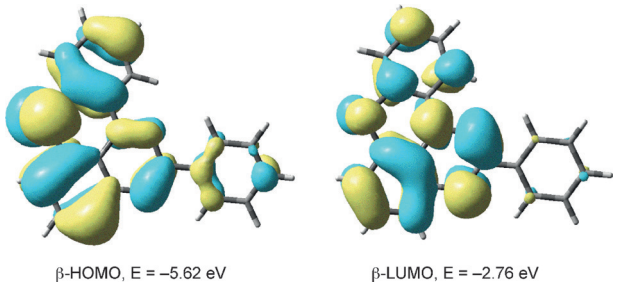

Figure 4. TD-DFT-derived contours for two MOs responsible for near-IR absorption in $\mathbf{1_S}$.

In contrast to the observed effects in UV/Vis spectra, peri-annulation of **1** has little impact on electrochemical behavior of the radicals (Figure 5 and Table 1). The only noticeable effect is observed for the reduction potential, $E_{1/2}{}^{-1/0}$, of the $\mathbf{1_S}$ which is shifted anodically by 0.12 V relative to that in **1**.

The electrochemical behavior of the radicals is consistent with the results of DFT calculations, which show that the adiabatic ionization potential, I_p, is nearly constant in the

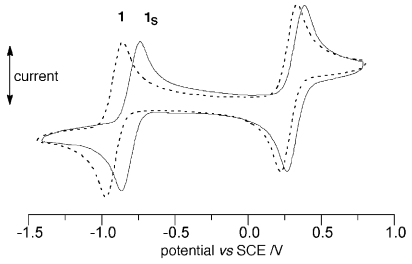

Figure 5. Cyclic voltammograms for Blatter radical (**1**, dotted line), and $\mathbf{1_S}$ (full line). Reaction conditions: 0.5 mM in CH_2Cl_2 $[nBu_4N]^+$ $[PF_6]^-$ (50 mM), ca. 20 °C, 50 mV s^{-1}, glassy carbon electrode.

Table 1: Cyclic voltammetry data[a] and calculated ionization potentials I_p and electron affinities E_a for radicals.[b]

Radical	$E_{1/2}^{-1/0}$ [V]	$E_{1/2}^{0/+1}$ [V]	E_{cell}[c] [V]	I_p [eV]	E_a [eV]
1	−0.92[d]	+0.28[d]	1.20[d]	5.83	−1.29
$\mathbf{1_S}$	−0.80	+0.33	1.13	5.89	−1.48
$\mathbf{1_O}$	−0.89	+0.31	1.20	5.74	−1.29

[a] Recorded in CH_2Cl_2 [n-Bu_4N]$^+$[PF_6]$^-$ (50 mM), ca. 20 °C, 50 mV s^{-1}, glassy carbon electrode and reported vs SCE. [b] E_a and adiabatic I_p calculated at the B3LYP/6-31G(2d,p) level of theory in vacuum. [c] $E_{cell} = E_{1/2}^{0/+1} - E_{1/2}^{-1/0}$. [d] From Ref. [12]. For details see the Supporting Information.

series, while the electron affinity, E_a, is higher by about 0.2 eV for $\mathbf{1_S}$ than that for either **1** or $\mathbf{1_O}$ (Table 1). The calculations also revealed that the disproportionation of the three radicals ($2R^{\bullet} \rightarrow R^+ + R^-$) is a relatively low-energy process ($\Delta E_{SCF} \approx 112$ kcal mol^{-1}) with the lowest relaxation energy for the oxygen analogue $\mathbf{1_O}$ ($\Delta\Delta E_{SCF} = -6.7$ kcal mol^{-1}) because of its C_s symmetry. Radicals with such favorable thermodynamics of the disproportionation process are sought after as molecular semiconductors.[18]

EPR spectroscopy (Figure 6) supported by DFT calculations revealed that as the planarization of the Blatter radical progresses, the spin density is drained mainly from N2 and, to a lesser extent, from N4 towards N1, and increases on the N1-Ph ring (Table 2; see the Supporting Information). This drain results in additional 7.9 and 9.1% of spin density being transferred from the benzo[*e*][1,2,4]triazinyl core to the N1-Ph ring in $\mathbf{1_S}$ and $\mathbf{1_O}$, respectively, relative to **1**. Thus, the total spin density, ρ, on the Ph ring increases from 0.058 in **1** to

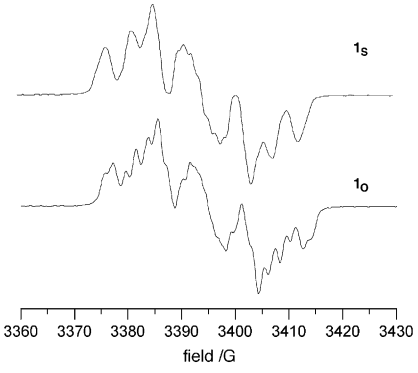

Figure 6. Experimental spectra for $\mathbf{1_S}$ (top) and $\mathbf{1_O}$ (bottom) recorded in CH_2Cl_2 at 23 °C. For the simulated spectra see the Supporting Information.

Table 2: Selected experimental and calculated hfcc a_N and spin densities ρ_N.[a]

Radical	a_{N1}/G, ρ_{N1}	a_{N2}/G, ρ_{N2}	a_{N4}/G, ρ_{N4}
1	7.65 (5.51), 0.255	4.87 (3.80), 0.293	4.90 (4.32), 0.292
$\mathbf{1_S}$	7.42 (5.62), 0.256	4.36 (3.48), 0.269	4.38 (3.95), 0.270
$\mathbf{1_O}$	7.59 (5.66), 0.281	4.14 (3.24), 0.245	4.36 (3.82), 0.258

[a] Experimental a_N values from simulation using all N and H atoms. Theoretical isotropic a_N values (in parentheses) and spin densities ρ_N obtained at the B3LYP/6-31++G(2d,p)// B3LYP/6-31G(2d,p) level of theory in CH_2Cl_2 dielectric medium. Numbering system adopted from **1**. For details see the Supporting Information.

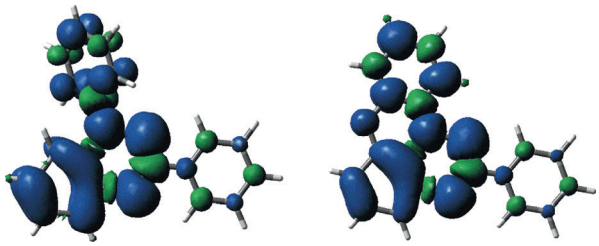

Figure 7. B3LYP/6-31++G(2d,p)// B3LYP/6-31G(2d,p)-derived spin densities for **1** (left) and its oxygen analogue $\mathbf{1_O}$ (right).

0.082 (plus $\rho_S = +0.036$) in $\mathbf{1_S}$ and 0.107 (plus $\rho_O = +0.029$) in $\mathbf{1_O}$ (Figure 7).

Lastly, the magnetic susceptibility of the two radicals was measured as a function of temperature in a range of 300→2 K at 0.60 T ($\mathbf{1_S}$) and 0.80 T ($\mathbf{1_O}$). Results show that both radicals exhibit nearly ideal paramagnetic behavior at high temperatures (>175 K, Figure 8). Measurements at lower temper-

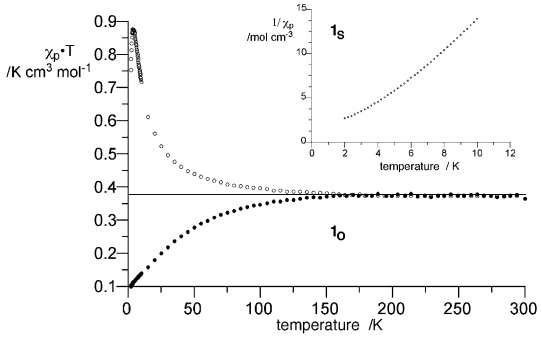

Figure 8. $\chi_p T$ vs. T plot in the range 300–2 K for $\mathbf{1_S}$ (upper, open circles) and $\mathbf{1_O}$ (lower, full circles). The inset shows the low temperature portion of the $1/\chi_p$ vs. T plot for $\mathbf{1_S}$. The horizontal line $\chi_p T = 0.375$ K cm^3 mol^{-1} represents behavior of an ideal paramagnet.

atures demonstrated increasing weak antiferromagnetic interactions in $\mathbf{1_O}$, essentially in the absence of any significant intermolecular close contacts. In contrast, the sulfur analogue $\mathbf{1_S}$ exhibits weak ferromagnetic interactions below 200 K, which, at 4.5 K are dominated by antiferromagnetic exchange interactions. Analysis of the crystal structure of $\mathbf{1_S}$ revealed that the puckered molecules are arranged into stacks, in which they are related by a twofold screw axis. This stacking results in the overlap of the [1,2,4]triazine and N1-Ph rings and significant close intermolecular contacts between two sites with positive spin densities [C3a···C9, $\Delta d = -0.107$ Å, $\rho_{C9} = +0.081$ and $\rho_{C3a} = +0.025$; Figure 2]. The observed molecular arrangement indicates that the ferromagnetic behavior of $\mathbf{1_S}$ can be approximated as one-dimensional Heisenberg ferromagnetic chain. Its modeling with Baker's high-temperature series expansion[19] yields the exchange coupling interaction energy $2J = 14.4$ cm^{-1}. This result is consistent with the DFT-calculated spin–spin exchange interaction $2J = 17.2$ cm^{-1}, determined as a difference between the SCF energies of the triplet (E_T) and broken singlet (E_{BS}) for a pair of neighboring molecules in the stack at their crystallographic coordinates. Similar calculations for two other molecular pairs revealed

that inter-stack close interactions [such as C9-H···N3 and C9-H···H-C(Ph)] are less significant for the observed magnetic behavior of the solid. Fitting of the magnetization vs field data, obtained at 2 K, $M(H)_{2K}$, with the Brillouin function indicates that the spin state responsible for the observed ferromagnetic behavior is $S = 3$ (see the Supporting Information).

In conclusion, we have demonstrated a simple and convenient two-step method for the preparation of fused-ring planar benzo[*e*][1,2,4]triazinyl radicals. The method is potentially general and by using appropriate 1-bromo(iodo)-2-hydroxy(mercapto)arenes it may provide access to a wealth of functionalized open-shell ring-fused structures containing the benzo[*e*]-[1,2,4]triazinyl unit with fully controlled spin delocalization, electronic absorption, and steric bulk of the substituents. In this respect, the method complements the previously developed ring annulations in area I of the Blatter radical and permits full steric and electronic control in the previously inaccessible for major structural modifications area II (Figure 9). Thus, structures $\mathbf{1_S}$ and $\mathbf{1_O}$ represent a new paradigm in the structural chemistry of Blatter radical and offer a new planar platform for molecular and supramolecular engineering in the context of magnetostructural studies, development of near-IR absorbing radicals for biomedical applications, molecular electronics, photovoltaics, and liquid crystals. Some of these newly opened avenues are being pursued in our laboratory.

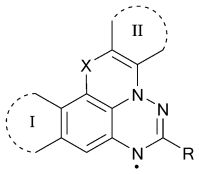

Figure 9. Expansion of spin delocalization in the benzo[*e*]-[1,2,4]triazinyl through peri-annulation: in area I (the known post radical modification methods) and in area II (the new method).

Acknowledgments

Support for this project was provided by the National Science Foundation (CHE-1214104) and National Science Center (2014/13/B/ST5/04525). Crystallographic data were collected by Dr. J. Krause through the SCrALS (Service Crystallography at the Advanced Light Source) program at the Advanced Light Source, Lawrence Berkeley National Laboratory under contract No. DE-AC02-05CH11231. C.P.C. thanks Prof. David A. Shultz for his hospitality and the use of his laboratory.

Keywords: magnetic properties · radicals · solid-state structure · structure elucidation · supramolecular chemistry

How to cite: *Angew. Chem. Int. Ed.* **2016**, *55*, 11149–11152
Angew. Chem. **2016**, *128*, 11315–11318

[1] a) R. G. Hicks, *Stable Radicals: Fundamentals and Applied Aspects of Odd-Electron Compounds*, Wiley, Chichester, **2010**; b) C. P. Constantinides, P. A. Koutentis, *Adv. Heterocycl. Chem.* **2016**, *119*, 173–207.

[2] F. A. Neugebauer, I. Umminger, *Chem. Ber.* **1981**, *114*, 2423–2430.

[3] F. A. Neugebauer, G. Rimmler, *Magn. Reson. Chem.* **1988**, *26*, 595–600.

[4] a) A. A. Berezin, G. Zissimou, C. P. Constantinides, Y. Beldjoudi, J. M. Rawson, P. A. Koutentis, *J. Org. Chem.* **2014**, *79*, 314–327; b) A. A. Berezin, C. P. Constantinides, S. I. Mirallai, M. Manoli, L. L. Cao, J. M. Rawson, P. A. Koutentis, *Org. Biomol. Chem.* **2013**, *11*, 6780–6795.

[5] a) F. A. Neugebauer, I. Umminger, *Chem. Ber.* **1980**, *113*, 1205–1225; b) A. Bodzioch, M. Zheng, P. Kaszyński, G. Utecht, *J. Org. Chem.* **2014**, *79*, 7294–7310.

[6] H. M. Blatter, H. Lukaszewski, *Tetrahedron Lett.* **1968**, *9*, 2701–2705.

[7] a) M. Demetriou, A. A. Berezin, P. A. Koutentis, T. Krasia-Christoforou, *Polym. Int.* **2014**, *63*, 674–679; b) J. Areephong, K. M. Mattson, N. J. Treat, S. O. Poelma, J. W. Kramer, H. A. Sprafke, A. A. Latimer, J. Read de Alaniz, C. J. Hawker, *Polym. Chem.* **2016**, *7*, 370–374.

[8] Y. Zhang, Y. Zheng, H. Zhou, M.-S. Miao, F. Wudl, T.-Q. Nguyen, *Adv. Mater.* **2015**, *27*, 7412–7419.

[9] Y. Zheng, M.-s. Miao, G. Dantelle, N. D. Eisenmenger, G. Wu, I. Yavuz, M. L. Chabinyc, K. N. Houk, F. Wudl, *Adv. Mater.* **2015**, *27*, 1718–1723.

[10] M. Jasiński, J. Szczytko, D. Pociecha, H. Monobe, P. Kaszyński, *J. Am. Chem. Soc.* **2016**, *138*, 9421–9424.

[11] P. A. Koutentis, D. Lo Re, *Synthesis* **2010**, 2075–2079.

[12] C. P. Constantinides, E. Obijalska, P. Kaszyński, *Org. Lett.* **2016**, *18*, 916–919.

[13] a) C. P. Constantinides, A. A. Berezin, M. Manoli, G. M. Leitus, G. A. Zissimou, M. Bendikov, J. M. Rawson, P. A. Koutentis, *Chem. Eur. J.* **2014**, *20*, 5388–5396; b) A. A. Berezin, C. P. Constantinides, C. Drouza, M. Manoli, P. A. Koutentis, *Org. Lett.* **2012**, *14*, 5586–5589; c) Y. Zheng, M.-s. Miao, M. C. Kemei, R. Seshadri, F. Wudl, *Isr. J. Chem.* **2014**, *54*, 774–778.

[14] Y. Miura, N. Yoshioka, *Chem. Phys. Lett.* **2015**, *626*, 11–14.

[15] a) C. P. Constantinides, P. A. Koutentis, J. M. Rawson, *Chem. Eur. J.* **2012**, *18*, 15433–15438; b) C. P. Constantinides, A. A. Berezin, M. Manoli, G. M. Leitus, M. Bendikov, J. M. Rawson, P. A. Koutentis, *New J. Chem.* **2014**, *38*, 949–954; c) C. P. Constantinides, A. A. Berezin, G. A. Zissimou, M. Manoli, G. M. Leitus, M. Bendikov, M. R. Probert, J. M. Rawson, P. A. Koutentis, *J. Am. Chem. Soc.* **2014**, *136*, 11906–11909.

[16] a) C. P. Constantinides, P. A. Koutentis, H. Krassos, J. M. Rawson, A. J. Tasiopoulos, *J. Org. Chem.* **2011**, *76*, 2798–2806; b) B. Yan, J. Cramen, R. McDonald, N. L. Frank, *Chem. Commun.* **2011**, *47*, 3201–3203; c) Y. Takahashi, Y. Miura, N. Yoshioka, *New J. Chem.* **2015**, *39*, 4783–4789.

[17] a) C. P. Constantinides, E. Carter, D. M. Murphy, M. Manoli, G. M. Leitus, M. Bendikov, J. M. Rawson, P. A. Koutentis, *Chem. Commun.* **2013**, *49*, 8662–8664; b) C. P. Constantinides, P. A. Koutentis, J. M. Rawson, *Chem. Eur. J.* **2012**, *18*, 7109–7116; c) A. T. Gubaidullin, B. I. Buzykin, I. A. Litvinov, G. N. Gazetdinova, *Russ. J. Gen. Chem.* **2004**, *74*, 939–943.

[18] For instance: a) R. C. Haddon, *Aust. J. Chem.* **1975**, *28*, 2343–2351; b) T. M. Barclay, A. W. Cordes, R. C. Haddon, M. E. Itkis, R. T. Oakley, R. W. Reed, H. Zhang, *J. Am. Chem. Soc.* **1999**, *121*, 969–976, and references therein; c) L. Beer, J. L. Brusso, A. W. Cordes, E. Godde, R. C. Haddon, M. E. Itkis, R. T. Oakley, R. W. Reed, *Chem. Commun.* **2002**, 2562–2563.

[19] G. A. Baker, Jr., G. S. Rushbrooke, H. E. Gilbert, *Phys. Rev.* **1964**, *135*, A1272–1277.

Received: June 9, 2016
Revised: July 7, 2016
Published online: August 11, 2016

